Hindawi
Journal of Chemistry
Volume 2020, Article ID 8651453, 9 pages
https://doi.org/10.1155/2020/8651453

Research Article

Fatty Acid Composition, Phospholipid Molecules, and Bioactivities of Lipids of the Mud Crab *Scylla paramamosain*

Thi Phuong Lan Nguyen[1,2] **Van Tuyen Anh Nguyen**[3] **Thi Thanh Trung Do**[3] **Trung Nguyen Quang**[4] **Quoc Long Pham**[3] **and Tat Thanh Le**[1,3]

[1]*Graduate University of Sciences and Technology, Vietnam Academy of Science and Technology (VAST), 18-Hoang Quoc Viet, Cau Giay, Hanoi, Vietnam*
[2]*Vietnam Food Administration, Ministry of Health, 138-Giang Vo, Ba Dinh, Hanoi, Vietnam*
[3]*Institute of Natural Products Chemistry, VAST, 18-Hoang Quoc Viet, Cau Giay, Hanoi, Vietnam*
[4]*Center for Research and Technology Transfer, VAST, 18-Hoang Quoc Viet, Cau Giay, Hanoi, Vietnam*

Correspondence should be addressed to Tat Thanh Le; thanh.biotech@gmail.com

Received 16 October 2019; Revised 10 February 2020; Accepted 13 February 2020; Published 19 March 2020

Academic Editor: Thomas R. Caulfield

The mud crab increases the yield of farming in Southeast Asian countries. *Scylla paramamosain*, one of four mud crab species belonging to the *Scylla* genus, is a rich nutrient source during its soft-shell moulting period. In this study, we analysed the total lipid content, fatty acid components, and phospholipid molecular species of the *S. paramamosain* mud crab. The total lipid content was 1.62 ± 0.08%, which is similar to that of *S. serrata* previously reported. Twenty-one fatty acids were identified in *S. paramamosain*. The composition and molecular forms of the phospholipids were identified using high-performance liquid chromatography-high-resolution mass spectrometry. Fifty-four different molecules belonging to six types of phospholipids were identified. Notably, phospholipids were made of fatty acids with C16 : 0; C18 : 0; C20 : 4; C20 : 5; and C22 : 6 main components. The anti-inflammatory and cytotoxic effects of crab lipids and phospholipids were investigated for the first time. The anti-inflammatory activity of the total and polar lipids had IC_{50} values of 71.5 and 68.6 μg/mL, respectively. The crab polar lipid fraction, which contained phospholipids, also presented high cytotoxic activity toward five cancer cell lines with IC_{50} values ranging from 85.4 to 95.8 μg/mL.

1. Introduction

Crab species of the genus *Scylla* are known as mud crabs and include the four species of *S. serrata* (Forskål), *S. tranquebarica* (Fabricius), *S. olivacea* (Herbst), and *S. paramamosain* (Estampador) [1]. These crabs are widely distributed in warm waters such as the tropical waters of the Indian and Pacific oceans [2]. The cultured mud crab is highly nutritious and is an important source of income for farmers in coastal communities because of the rising demand for crab meat in both domestic and export markets. *S. paramamosain* has been studied in Thailand and China and is the most common species of mud crab in Vietnam [3–5]. However, there have been no studies of this crab during its moulting period, which is an important aspect of the crab life cycle that creates a special kind of crab, i.e., soft-shell crab.

A soft-shell crab is the physiological form of any crab after moulting when the crab replaces its old skeleton with a new, larger, and decalcified soft skeleton. Soft-shell crab is very nutritious with high mineral, protein, and healthy fatty acid contents [6]. Lipids are an important nutrient source for the growth of organisms, especially crustaceans, because they are precursors of hormones that promote the moulting process [7, 8]. Phospholipids, which are lipid components, are believed to affect the growth and metabolism of crabs [9, 10]. The phospholipid content of crustaceans typically ranges from 1% to 3% [11]. The absence of phospholipids in the diet is detrimental to crustaceans and results in moult

death syndrome, which is indicated by death during or suddenly after moulting [12]. In the crab structure, phospholipids maintain the structural integrity of biological membranes and are precursors of important steroids [13].

Phospholipids are also essential for human dietary because their fatty acid residues are delivered to incorporate with cell membrane after digestion and absorption in the intestinal lumen [14]. Phospholipids consist of phosphatidylethanolamine, phosphatidylinositol, phosphatidylserine, and phosphatidylcholine, in which, phosphatidylcholine is most abundant with more than 50% of phospholipid content in the intestine [15]. Phospholipid was shown multi-bioactivities in human, such as anti-inflammat anti-inflammatory, anticancer, and antitumor activities. Recent studies indicated that the fatty acid composition of phospholipids has decided their bioactivity [16, 17]. In report of Gaudry, 2014, prostate cancer patients took marine phospholipid containing high omega-3 fatty acids and evaluated the effect on the disease treatment [16]. This demonstrated that marine phospholipids were effective in increasing the n-3/n-6FA ratio significantly in cells and reducing the biosynthesis of proinflammatory eicosanoids in tumor cells, thus reducing metastatic progression of prostate cancer and inhibiting inflammation [14, 16, 17].

Herein, we detail the total lipids, fatty acids, and phospholipids present in soft-shell mud crabs found in Vietnam. Many molecular types were characterised. This study also evaluated the anti-inflammatory and cytotoxic activities of the polar and neutral lipid fractions; the polar lipid fraction contained the phospholipids.

2. Materials and Methods

2.1. Lipid Extraction and Fractionation. Samples of *S. paramamosain* were collected at an experimental farm by Dr. Bui Thi Bich Ngoc, the Research Institute for Aquaculture No. 3. The moulting crab weight ranged from 100 to 110 g. Crabs were peeled within 2 h of collection, frozen, and transferred to the Institute of Natural Products Chemistry. Lipids were extracted from the crab samples according to the methods of Bligh and Dyer in combination with ultrasound [18, 19]. A sample (10 g) was ground and added to 30 mL of methanol-chloroform (MeOH-$CHCl_3$; 2 : 1 v/v). The mixture was then exposed to three successive 30-minute ultrasound treatments. Filtration provided the first solution, and the residue was soaked in 10 mL $CHCl_3$ and the ultrasound treatment was repeated. The second solution after filtering was combined with the first solution, and 8 mL of water (H_2O) was added. The resulting solution was vigorously shaken and transferred to a separating funnel. The lower organic phase containing the lipids was treated with Na_2SO_4 to absorb H_2O. Then, this anhydrous phase was filtered and evaporated to dryness to provide the total lipids. The total lipids were dissolved in $CHCl_3$ and stored at −5°C. An aliquot of this total lipid solution (200 mg) was dissolved in $CHCl_3$ and fractionated on silica columns (J. T. Baker, Phillipsburg, NJ, USA). The silica gel was saturated with $CHCl_3$, and the lipid aliquot was applied to the column. Chloroform (32 mL) was used to elute the neutral lipids, and four column volumes (56 mL) of MeOH-H_2O (97 : 3 v/v) were used to elute the polar lipids, which contained the phospholipids. The obtained fractions were dried in Ar gas and stored at −35°C until analysed.

2.2. Fatty Acid Analysis. Fatty acid methyl esters (FAMEs) were obtained by treating the lipids with 2% H_2SO_4 in CH_3OH and incubating at 80°C for 2 h. Then, n-hexane (2 mL) and H_2O (0.1 mL) were added, and the solution was vigorously shaken. The upper organic phase was purified by thin-layer chromatography using hexane : diethyl ether (95 : 5 v/v). The FAME content was determined by gas chromatography at 210°C using a Shimadzu GC-2010 (Kyoto, Japan) instrument equipped with a flame ionisation detector on an Equity 5 capillary GC column (Merck; length × internal diameter = 30 $m \times 0.25$ mm; film thickness = 0.25 μm). Helium was used as the carrier gas at 20 mL/min. The initial oven temperature of 160°C was ramped at 2°C/min to 240°C and held at this temperature for 20 min. The injector and detector temperatures were maintained at 250°C [20]. FAMEs were analysed by gas chromatography-mass spectrometry (GC-MS) to identify the fatty acid structures. The spectra were compared with the NIST library and fatty acid mass spectra archive [21].

2.3. Analysis of the Molecular Species of Phospholipids. The chemical structures and relative amounts of molecular species of phospholipids were analysed by high-performance liquid chromatography-high resolution mass spectrometry (HPLC-HRMS). Phospholipids were separated from the polar lipid fraction using HPLC using a solvent system with a constant triethylamine [$(C_2H_5)_3N$] content, i.e., $(C_2H_5)_3$ N/formic acid (0.08 : 1, v/v) [22]. This provided suitable electrospray ionisation (ESI) conditions and a stable ion signal with the simultaneous registration of positive and negative ions. Polar lipids of *S. paramamosain* were analysed using gradient solvent mixtures, i.e., A: *n*-hexane/2-propanol/formic acid/$(C_2H_5)_3N$ (82 : 17 : 1 : 0.08, v/v/v/v) and B: 2-propanol/H_2O/formic acid/$(C_2H_5)_3N$ (85 : 14 : 1 : 0.08, v/v/v/v). The gradient began with 5% of mixture B and its percentage increased to 80% over 25 min. This composition was maintained for 1 min before returning to 5% of mixture B over 10 min when it was maintained at 5% for another 4 min (total run time was 40 min). The flow rate was 0.2 mL/min. Polar lipids were analysed by HRMS with processing software (LC Solutions ver. 3.60.361, Shimadzu). Quantification of the individual molecular species within each polar lipid class was carried out by calculating the peak areas of the individual extracted ion chromatograms [23].

2.4. Assay for Inhibition of Nitric Oxide Production. Lipopolysaccharide (LPS) from *Escherichia coli*, sodium nitrite, sulphanilamide, N-1-napthylethylenediamine dihydrochloride, and dimethyl sulphoxide (DMSO) were obtained from Sigma (St. Louis, MO, USA). Dulbecco's Modified Eagle's Medium and foetal bovine serum were purchased from Life Technologies (Carlsbad, CA, USA). RAW 264.7 cells were provided by Prof. Chi-Ying Huang, Yangming University, Taiwan.

The nitric oxide (NO) assay was performed as described previously with slight modification [24]. Following pre-incubation of RAW 264.7 cells (2×10^5 cells/mL) with LPS (1 μg/mL) for 24 h, the quantity of nitrite in the culture medium was measured as an indicator of NO production. Amounts of nitrite, a stable metabolite of NO, were measured using Griess reagent (1% sulphanilamide and 0.1% naphthylethylenediamine dihydrochloride in 2.5% phosphoric acid). In brief, 100 μL of cell culture medium was mixed with 100 μL of Griess reagent. Subsequently, the mixture was incubated at room temperature for 10 min and the absorbance at 540 nm was measured in a microplate reader. Fresh culture medium was used as a blank in every experiment. The quantity of nitrite was determined from a sodium nitrite standard curve.

Cell viability was determined by the 3-(4,5-dimethylthiazol-2-yl)-2,5-diphenyltetrazolium bromide (MTT) uptake method. First, 180 μL of RAW 264.7 cells at suitable concentration were dropped into 96-well plates in the presence of lipid extracts at concentrations of 100 μg/mL and then incubated at 37°C with 5% CO_2. After 72 h, MTT (5 μg/mL) was added to the medium for 4 h. Finally, the supernatant was removed and the formazan crystals were dissolved in DMSO. Absorbance was measured at 540 nm. The percentage of dead cells was determined relative to the control samples.

2.5. Cytotoxicity Assay with Five Cancer Cell Lines. Cytotoxicity of the lipid sample was evaluated against five human cancer cell lines using the sulphorhodamine B (SRB) cytotoxicity assay [25]. Five cancer cell lines were SK-LU-1 human lung cancer cell line, HL-60 human leukemia cell line, HT-29 human colon cancer cell line, HepG2 human liver cancer cell line, and MCF7 human breast cancer cell line whichprovided by Prof. Dr. D.V. Delfino, Perugia University, Italy. Each cancer cell line was trypsinised and incubated with lipid samples at concentrations of 0.8, 4, 20, and 100 μg/mL in 96-well plates at 37°C for 48 h. Following this, cells were fixed with trichloroacetic acid for 1 h at room temperature (28 ± 2°C). SRB solution (100 μL of 0.4% w/v in 1% acetic acid) was added to each well. After 30 min, the unbound SRB was removed by washing with 1% acetic acid. The samples were then air-dried at room temperature (28 ± 2°C). The protein bound stain was solubilised with 10 mM Tris base (pH 10.2), and the absorbance was measured at 515 nm using a microplate reader (SpectraMax Plus 384; Molecular Devices, Sunnyvale, CA, USA).

3. Results

3.1. Total Lipid Content and Fatty Acid Components. The total lipid (TL) content of *S. paramamosain* was 1.62 ± 0.08%. This result is similar to that of *S. serrata* [26, 27]. The fatty acid composition is given in Table 1. The identified 21 fatty acids contained 14 to 22 carbon atoms. The amounts of 16 : 0, 18 : 1(n−9), and 18 : 2(n−6) fatty acids were 18.58%, 25.70%, and 15.26%, respectively, which were higher than those reported elsewhere. By contrast, the contents of other important fatty acids were lower than those previously reported, i.e., 1.59%, 4.55%, and 7.19% for 20 : 4(n−6) (ARA), 20 : 5(n−3) (EPA), and 22 : 6(n−3) (DHA), respectively [26, 27]. The fatty acids were divided into saturated fatty acids (SAFAs), monounsaturated fatty acids (MUFAs), and polyunsaturated fatty acids (PUFAs) with average contents of 28.11%, 34.79%, and 31.77%, respectively. SAFAs contained the two major fatty acids of C16 : 0 and C18 : 0 (18.58% and 5.06%). MUFA content was mainly C18 : 1(n−9), which at 25.70% was the most abundant fatty acid among the 21 identified fatty acids. In the PUFA group, the C18 and C20 long-chain fatty acids had the same total contents. This differed from other studies on animal fatty acids that found a much higher C20 content than C18 content.

Table 1: Fatty acid composition (% of total) of *S. paramamosain*.

No	RT (min)	FA	Area	Content (%)
∑SAFAs			2462627.43	28.11
1	3.751	14 : 0	209409.20	2.39
2	4.47	15 : 0	42628.14	0.49
3	5.533	16 : 0	1628451.29	18.58
4	6.816	17 : 0	46015.09	0.53
5	8.738	18 : 0	443135.35	5.06
6	14.577	20 : 0	26656.91	0.30
7	26.671	22 : 0	66331.46	0.76
∑*MUFAs*			**3049461.26**	**34.79**
8	5.875	16:1n-7	311032.78	3.55
9	7.283	17:1n-7	41562.50	0.47
10	7.676	17:1n-5	10741.62	0.12
11	9.414	18:1n-9	2252025.61	25.70
12	9.491	18:1n-7	238175.18	2.72
13	15.35	20:1n-11	80715.78	0.92
14	15.551	20:1n-9	115207.78	1.31
∑*PUFAs*			**2783972.03**	**31.77**
15	10.591	18:2n-6	1336831.75	15.26
16	12.411	18:3n-3	128126.86	1.46
17	17.765	20:2n-6	55195.55	0.63
18	20.598	20:4n-6	139728.98	1.59
19	24.96	20:5n-3	398644.12	4.55
20	44.207	22:5n-3	95623.15	1.09
21	48.53	22:6n-3	629821.62	7.19
*Others**			**466473.68**	**5.33**

*Others include t16:1n-7; i17 : 0; a17 : 0; phytanic; i18 : 0; 14:1n-5; 15:1n-7; 15:1n-5; 16:1n-5; 18:1n-5; 20:1n-7; 18:4n-3; 20:3n-6; 20:4n-3; 21:3n-6; 21:4n-6; 21:5n-3; 22:4n-6; 22:5n-6; DMA. SAFAs: saturated fatty acids; MUFAs: monounsaturated fatty acids; PUFAs: polyunsaturated fatty acids.

3.2. Molecular Species of Phospholipids. Phospholipids form the basis of cellular structures. Because of their amphiphilic properties, they have a natural tendency to form bilayers in aqueous systems [28]. The phospholipid structure was determined using the HRMS fragmentation data of phospholipid standards as described previously [20]. In *S. paramamosain*, the content of polar lipids containing glycolipids and phospholipids was 40.02% of the total lipids. Glycolipids are the main component of photosynthetic organelles in plants, while phospholipids are present in the cell membranes of both animals and plants [29, 30]. In this study, we focused on determining phospholipid structures using molecular analysis. There were six types of

molecular species of phospholipids present in the TL fraction of *S. paramamosain*: phosphatidylethanolamine (PE), lysophosphatidylethanolamine (LPE), phosphatidylinositol (PI), phosphatidylserine (PS), phosphatidylcholine (PC), and lysophosphatidylcholine (LPC) (Figure 1).

For ethanolamine glycerophospholipid or PE, the ESI-HMRS signals of negative ions and corresponding positive ions were analysed simultaneously [19, 20]. The negative fragment ion signal was always more intense than that of the positive ion (Figure 1S). Four PE molecules were identified in the polar lipids of *S. paramamosain*. The most intense signal in the MS^- spectrum of PE was 39.12% at *m/z* 748.5128, which corresponded to the positive ion signal at *m/z* 750.5464. The empirical formula thus corresponded to $C_{43}H_{76}NO_7P$ (different by 0.01536 mass units; eight double bonds) as the first type of alkenyl acyl PE.

Three signals were observed in the MS^{2-} spectrum: *m/z* 301.2141 corresponding to the ion of the C20 : 5 acid and two signals at *m/z* 283.2101 and 257.2249 for ion fragments of the C20 : 5 acid that had lost an H_2O molecule and CO_2 molecule, respectively. The fragment at *m/z* 464.3115 corresponded to the PE molecule that had lost the $C_{20}H_{28}O$ neutral fragment, i.e., $C_{19}H_{29}COOH–H_2O$. Thus, this PE form contained an 18:0p alkenyl radical. These data established that the PE molecule was alkenyl acyl PE 18:0p/20 : 5.

The second type of alkenyl acyl PE was found at *m/z* 774.5244 (28.39%) (Table 2). It corresponded to the empirical formula $C_{45}H_{78}NO_7P$ (different by 0.01841; nine double bonds). Signals at *m/z* 327.2275 and 283.2388 in the MS^- spectrum corresponded to the ion fragments of the C22 : 6 acid and the ion fragment of the C22 : 6 acid that had lost a CO_2 molecule, respectively. The signals at *m/z* 446.3010 and 464.3104 corresponded, respectively, to the ion fragments of the PE molecule that had lost the C22 : 6 acid fragment and to the neutral fragment $C_{22}H_{30}O$ (i.e., $C_{21}H_{31}COOH–H_2O$). The ion fragment of the remaining alkenyl was thus C18:0p. It can be indicated that the second type of PE molecule referred to the alkenyl acyl 18:0p/22 : 6.

The first form of diacyl PE (30.03%) displayed the most intense signal at *m/z* 762.4949, which corresponded to the calculated formula of $C_{43}H_{74}NO_8P$ (different by 0.01103; nine double bonds). The MS^{2-} spectrum of this PE molecule displayed signals of fragments at *m/z* 255.2329 and *m/z* 327.2295 corresponding to a couple of ion fragments C16 : 0 acid/C22 : 6 acid, respectively (Figure 2S). The remaining fragments were observed at *m/z* 283.2489, corresponding to the ion of the C22 : 6 acid that had lost a CO_2 molecule, and at *m/z* 452.2760, corresponding to the PE molecular ion that had lost the neutral fragment $C_{22}H_{30}O$ (i.e., $C_{21}H_{31}COOH–H_2O$). Besides, on the same MS^{2-} spectrum, we obtained a fragment signal of C18 : 1 acid at *m/z* 281.2474 and a signal of C20 : 5 acid at *m/z* 301.2139. Thus, the observed ion fragments indicated this PE form contained two molecule types of the diacyl 16 : 0/22 : 6 and the diacyl 18 : 1/20 : 5.

The second diacyl form was identified as PE 16 : 0/18 : 1; it had the lowest content of 2.46% (Table 2). The MS^-spectrum displayed an ion fragment at *m/z* 716.5199 that corresponded to the empirical formula $C_{39}H_{76}NO_8P$ (different by 0.00558; four double bonds). The MS^{2-} spectrum displayed signals at *m/z* 281.2429 corresponding to the ion of the C18 : 1 acid, at *m/z* 255.2318 corresponding to the ion of the C16 : 0 acid, and at *m/z* 452.2781 corresponding to the PE molecular ion that had lost the neutral fragment $C_{18}H_{32}O$ (i.e., $C_{17}H_{31}COOH–H_2O$).

Lyso ethanolamine glycerophospholipid or LPE forms resemble PE, but a hydrogen atom is present instead of an acyl or alkyl/alkenyl radical. Three molecules with different concentrations were observed. The first LPE form with the highest content of 50.89% in the MS^-spectrum appeared at *m/z* 498.2585 and corresponded to the empirical formula $C_{25}H_{42}NO_7P$ (different by 0.00411; seven double bonds) (Table 3). Signals at *m/z* 301.2149, 283.2101, and 257.2252 in the MS^{2-} spectrum corresponded to ion fragments of the C20 : 5 acid and of the C20 : 5 acid that had lost H_2O and CO_2 molecules, respectively (Figure 3S). The first LPE form thus contained the 20 : 5 fatty acid.

The second LPE with a content of 32.84% displayed signals at *m/z* 524.2716 in the MS^-spectrum. This signal corresponded to formula $C_{27}H_{44}NO_7P$ (different by 0.00666; eight double bonds). The MS^{2-} spectrum displayed two signals at *m/z* 327.2290 and 283.2390, which corresponded to ion fragments of the C22 : 6 acid and of the C22 : 6 acid that had lost a CO_2 molecule. These results indicated that the second LPE molecule had the 22 : 6 fatty acid.

The final LPE with the lowest content of 16.28% displayed an MS^- signal at *m/z* 500.2719, which corresponded to the empirical formula $C_{25}H_{44}NO_7P$ (different by 0.00586; six double bonds). The MS^{2-} spectrum displayed four ion fragments, i.e., two fragments at *m/z* 303.2290 and *m/z* 259.2420, respectively, corresponding to ion fragments of the C20 : 4 acid and of the C20 : 4 acid that had lost a CO_2 molecule. Thus, the final LPE had the structure with C20 : 4 acid. The $MS^-$and MS^{2-} data thus indicated that all three LPE forms lost the acyl radical and then continued to lose a CO_2 molecule.

Negative ion $[M–H]^-$ signals corresponding to inositol glycerophospholipid or PI were observed in the ESI-MS1 spectra. Many signals of different fragments were observed in the MS^{2-} spectrum, of which some corresponded to the initial molecular ions that had lost small fragments such as a fatty acid molecule, a ketone radical, two fatty acids, or an inositol branch ($C_6H_{10}O_5$). In addition to signals of the PI ions, we always observed signals corresponding to two fatty acid ions derived from the PI molecule.

The most intense signal in the MS^-spectrum of the PI class appeared at *m/z* 883.5236 and corresponded to the empirical formula $C_{47}H_{81}O_{13}P$. The number of oxygen atoms in the formula indicated that the PI molecule had the diacyl form. The MS^{2-} spectrum displayed signals at *m/z* 281.2461 and 581.3024, which corresponded to the ion of the C18 : 0 acid and to the PI molecule that had lost the anion of the C20 : 5 acid, respectively. The signal at *m/z* 297.0349 corresponded to the $[C_9H_{14}O_9P]$ fragment, which was formed when the PI molecule lost two fatty acids. This specific ion fragment signal was characteristic of the PI class. Based on the obtained ion fragments (Figure 4S), the PI molecular structure was identified as PI 18 : 0/20 : 5.

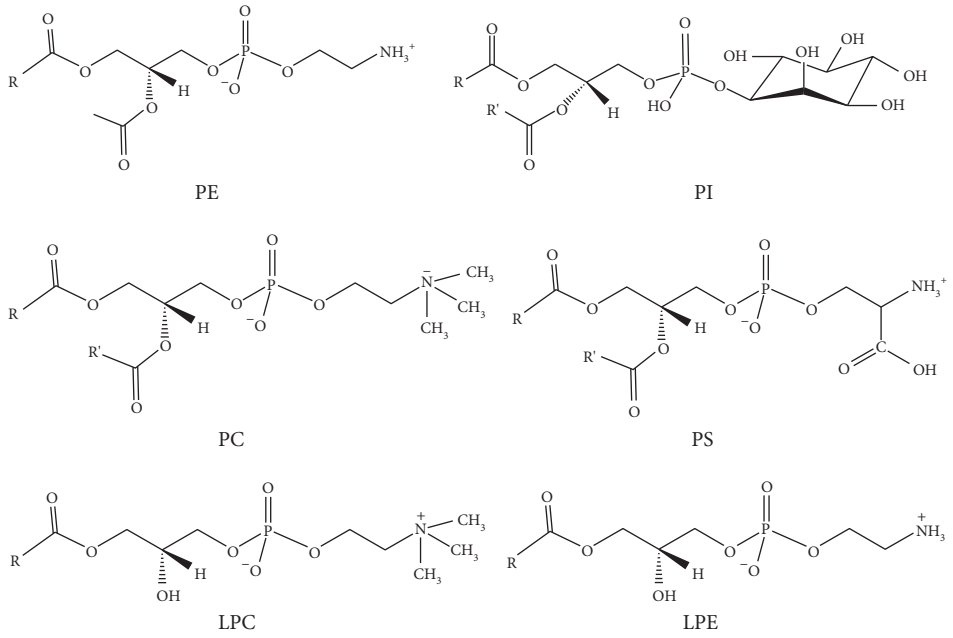

Figure 1: Structural formula of phospholipid classes.

Table 2: Molecular species of PE.

No	Species	Symbol	M^-	Formula	Area	% area in PE
1	PE 38 : 5	18:0p/20 : 5	748.5133	C_{43} H_{76} N O_7 P	212700087	39.12
2	PE 40 : 6	18:0p/22 : 6	774.5244	C_{45} H_{78} N O_7 P	154339310	28.39
3	PE 38 : 6	16 : 0/22 : 6 18 : 1/20 : 5	762.4969	C_{43} H_{74} N O_8 P	163242004	30.03
4	PE 34 : 1	16 : 0/18 : 1	716.5199	C_{39} H_{76} N O_8 P	13378702	2.46

Table 3: Molecular species of LPE.

No	Species	Symbol	M^-	Formula	Area	% area in PE
1	LPE 20 : 4	/20 : 4	498.2585	C_{25} H_{44} N O_7 P	284704668	50.89
2	LPE 20 : 5	/20 : 5	500.2719	C_{25} H_{42} N O_7 P	91064794	16.28
3	LPE 20 : 6	/22 : 6	524.2716	C_{27} H_{44} N O_7 P	183719085	32.84

Nine other PI molecules were similarly identified. Of these, PI 18 : 0/20 : 4 was the most abundant at 26.24% (Table 4). The second-, third-, and fourth-ranked positions belonged to PI 19 : 0/20 : 4 and PI 18 : 1/20 : 5 with contents of 18.40% and 11.89%, respectively. The remaining molecules had contents that were less than 10%. Notably, all PI molecules except PI 18 : 0/21 : 4 always contained a long-chain acyl 20 C tail with four or five double bonds.

The MS^{2-} spectra of serine glycerophospholipid and PS compounds always showed the loss of the neutral fragment corresponding to the serine group $C_3H_5NO_2$ (calculated *m/z* 87.0320) from the $[M–H]^-$ ions. This is a characteristic signal of PS molecules in ESI-MS spectra. In the ESI-MS spectra of the PS class of *S. paramamosain*, the most intense signals appeared at *m/z* 808.4996, corresponding to the empirical formula $C_{44}H_{76}NO_{10}P$ with nine double bonds. The number of oxygen atoms in these formulations established that both of the PS molecules contained two acyl groups. The MS^{2-} spectrum displayed typical fragments that included ion fragments of PS molecules that had lost the serine group ($C_3H_5NO_2$) and one fatty acid $[RCOO]^-$ or one ketone group $[R–CH=C=O]^-$. Specifically, the MS^{2-} spectral peak observed at *m/z* 301.2084 corresponded to the ion of the 20 : 5 acid and those at *m/z* 283.2617 and 257.2222 corresponded to the 20 : 5 acid that had lost one H_2O and CO_2 molecule, respectively. The appearance of two ion fragments at *m/z* 419.2523 and 437.2630 indicated that the PS molecule had lost serine group and 20 : 5 acid or ketone radical fragments. Figure 5S shows the MS^{2-} spectrum in detail. These results established that the PS molecule had the PS 18 : 0/20 : 5 structure.

We also identified 12 different types of PS molecules in the polar lipid fraction. The remaining form had low content (<10%) excepting the signal at *m/z* 810.5141 with content of 28.08% (Table 5).

For choline glycerophospholipid or PC, the MS^+ spectra showed characteristic signals of positive ions $[M + H]^+$ while the MS^- spectra displayed signals

Table 4: Molecular species of PI.

No	Species	Symbol	M^-	Formula	Area	% area in PE
1	PI 38 : 4	18 : 0/20 : 4	885.5431	C_{47} H_{83} O_{13} P	472261560	26.24
2	PI 38 : 5	18 : 0/20 : 5	883.5236	C_{47} H_{81} O_{13} P	502809634	27.94
3	PI 39 : 4	19 : 0/20 : 4	897.5343	C_{48} H_{83} O_{13} P	331172003	18.40
4	PI 38 : 6	18 : 1/20 : 5	881.5136	C_{47} H_{79} O_{13} P	213993221	11.89
5	PI 36 : 5	16 : 0/20 : 5	855.4930	C_{45} H_{77} O_{13} P	177410703	9.86
6	PI 38 : 4	18:0p/20 : 4	871.5200	C_{47} H_{85} O_{12} P	26375177	1.47
7	PI 30 : 4	16 : 0/20 : 4	857.5110	C_{45} H_{79} O_{13} P	21994467	1.22
8	PI 36 : 4	16:0p/20 : 4	843.5303	C_{45} H_{81} O_{12} P	18550087	1.03
9	PI 38 : 7	18 : 2/20 : 5	879.4933	C_{47} H_{77} O_{13} P	17794312	0.99
10	PI 39 : 4	18 : 0/21 : 4	899.5523	C_{48} H_{85} O_{13} P	17563605	0.98

Table 5: Molecular species of PS.

No	Species	Symbol	M^-	Formula	Area	% area in PE
1	PS 38 : 5	18 : 0/20 : 5	808.4996	C_{44} H_{76} N O_{10} P	370366219	31.23
2	PS 38 : 4	18 : 0/20 : 4	810.5141	C_{44} H_{78} N O_{10} P	332902308	28.08
3	PS 36 : 1	18 : 0/18 : 1	788.5366	C_{42} H_{80} N O_{10} P	95760000	8.08
4	PS 38 : 6	18 : 0/22 : 6	834.5133	C_{46} H_{78} N O_{10} P	90612835	7.64
5	PS 38 : 6	16 : 0/22 : 6	806.4873	C_{44} H_{74} N O_{10} P	75226947	6.34
6	PS 34 : 4	16 : 0/20 : 4	782.4886	C_{42} H_{74} N O_{10} P	48771734	4.11
7	PS 38 : 5	18 : 0/20 : 5	836.5266	C_{46} H_{80} N O_{10} P	44220009	3.73
8	PS 34 : 5	16 : 0/20 : 5	780.4749	C_{42} H_{72} N O_{10} P	34248519	2.89
9	PS 39 : 4	18 : 0/21 : 4 19 : 0/20 : 4	824.5275	C_{45} H_{80} N O_{10} P	25687559	2.17
10	PS 37 : 5	17 : 0/20 : 5	794.4896	C_{43} H_{74} N O_{10} P	23487115	1.98
11	PS 34 : 1	16 : 0/18 : 1	760.5086	C_{40} H_{76} N O_{10} P	18010699	1.52
12	PS 38 : 2	18 : 0/20 : 2	814.5435	C_{44} H_{82} N O_{10} P	14227570	1.20
13	PS 38 : 7	18 : 1/22 : 6	832.4979	C_{46} H_{76} N O_{10} P	12222509	1.03

corresponding to the two negative ions $[M + CH_3COO]^-$ and $[M–CH_3]^-$. This ion fragment was always selected for analysis in the MS^{2-} spectrum (Figure 6S). A strong signal corresponding to the $[M + CH_3COOX]^-$ ion was always present in the MS^{2-} spectrum of the $[M + CH_3COO]^-$ ion; it formed when the $[M + CH_3COO]^-$ ion lost a CH_3COOCH_3 molecule.

The various MS^+ and MS^-spectra enabled identification of 21 types of molecules belonging to the PC class (Table 6). Notably, the most intense signal at *m/z* 760.5906 in the MS^+ spectrum (10.59%) corresponded to the empirical formula $C_{42}H_{82}NO_8P$ (different by 0.00582; four double bonds). This was the first form of diacyl PC to be identified in this sample with both C16 : 0 and C18 : 1 fatty acids. The MS^{2-} spectrum displayed signals corresponding to fragments of the C18 : 1 acid at *m/z* 281.2479 and the C16 : 0 acid at *m/z* 255.2276. The signal at *m/z* 480.3151 corresponded to an ion fragment of PC that had lost a ketone group and a methyl group, i.e., M–[R–CH=C=O]–CH_3. Based on the observed fragments, the PC molecule was identified as the diacyl PC 16 : 0/18 : 1. Seven of the 21 identified molecular forms were similarly characterised using the MS^{2-} spectrum. Table 6 lists the PC molecules.

The LPC class has a similar structure as that of the PC group, but a hydrogen atom is present instead of an alkyl/alkenyl group. The LPC molecules were identified from the signals corresponding to the $[M–CH_3]^-$ and $[M–RCOO]^-$ ions in the MS^-spectrum. Of these, the LPC 20 : 5 molecule was characterised by the signal at *m/z* 526.2520; it had the highest content of 43.36%. This signal corresponded to the empirical formula $C_{28}H_{48}NO_7P$ (different by 0.00536; five double bonds). The MS^{2-} spectrum displayed peaks at *m/z* 301.2146 corresponding to the anion of the C20 : 5 acid and *m/z* 283.2101 and 257.2242 corresponding to the C20 : 5 acid that had lost a H_2O and CO_2 molecule, respectively (Figure 7S).

The LPC molecule with a second-ranked content of 38.00% had the structure 22 : 6. It displayed a signal at *m/z* 552.2672, which corresponded to the calculated formula $C_{30}H_{50}NO_7P$ (different by 0.00485; six double bonds). The last LPC molecule with the lowest content of 18.64% contained the 20 : 4 acid, which corresponded to the formula $C_{28}H_{52}NO_7P$. Table 7 provides the data that were used to identify the LPC molecules.

3.3. Anti-Inflammatory Activity. Lipids play important roles in many organisms. We wanted to study the impact of lipid components on human health. We first studied the biological activity of the neutralised and polar lipids; the latter contained phospholipids. Proinflammatory agents, such as LPS, can significantly increase the number of macrophages that produce NO [31, 32]. High levels of NO cause a variety of pathophysiological processes including inflammation [33] and carcinogenesis [34]. In this study, we evaluated the NO inhibitory activity of lipid fractions using an LPS-stimulated RAW 264.7 cell assay.

Table 6: Molecular species of PC.

No	Species	Symbol	M^+	Formula	Area	% area in PE
1	PC 34 : 1	16 : 0/18 : 1	760.5906	C_{42} H_{82} N O_8 P	73666078	10.59
2	PC 38 : 6	16 : 0/22 : 6	806.5697	C_{46} H_{80} N O_8 P	68048989	9.78
3	PC 38 : 5	18:0a/20 : 5	794.6093	C_{46} H_{84} N O_7 P	48890140	7.03
4	PC 38 : 4	18:0a/20 : 4	796.6281	C_{46} H_{86} N O_7 P	47673588	6.85
5	PC 38 : 6	18:0a/22 : 6	820.6168	C_{48} H_{86} N O_7 P	42015599	6.04
6	PC 38 : 6	18:1a/20 : 5 16:0a/22 : 6	792.5906	C_{46} H_{82} N O_7 P	36772078	5.28
7	PC 32 : 1	16 : 0/16 : 1 14 : 0/18 : 1	732.5603	C_{40} H_{78} N O_8 P	22786557	3.27
8	PC 37 : 5	37//5	780.5946	C_{45} H_{82} N O_7 P	41324220	5.94
9	PC 36 : 3	36//2	786.6018	C_{44} H_{84} N O_8 P	41375774	5.95
10	PC 36 : 4	36//4	782.5723	C_{44} H_{80} N O_8 P	39531943	5.68
11	PC 36 : 1	36//1	788.6132	C_{44} H_{86} N O_8 P	34925789	5.02
12	PC 36 : 5	36//5	766.5802	C_{44} H_{80} N O_7 P	31424839	4.52
13	PC 30 : 0	30//0	706.5426	C_{38} H_{76} N O_8 P	31193242	4.48
14	PC 38 : 5	38//5	808.5830	C_{46} H_{82} N O_8 P	27868540	4.00
15	PC 36 : 3	36//3	784.5861	C_{44} H_{82} N O_8 P	26587588	3.82
16	PC 36 : 1	36//1	774.6435	C_{44} H_{88} N O_7 P	25318478	3.64
17	PC 40 : 6	40//6	834.5995	C_{48} H_{84} N O_8 P	19216989	2.76
18	PC 48 : 7	40//7	832.5820	C_{48} H_{82} N O_8 P	14818070	2.13
19	PC 36 : 2	36//2	772.6299	C_{44} H_{86} N O_7 P	12130968	1.74
20	PC 40 : 7	40//7	818.6050	C_{48} H_{84} N O_7 P	8127222	1.17
21	PC 35 : 8	35//8	746.5136	C_{43} H_{72} N O_7 P	2162515	0.31

Table 7: Molecular species of LPC.

No	Species	Symbol	$[M\text{-}CH_3]^-$	Formula	Area	% area in PE
1	LPC 20 : 5	/20 : 5	526.2520	$C_{28}H_{48}NO_7P$	202270433	43.36
2	LPC 20 : 6	/22 : 6	552.2672	$C_{30}H_{50}NO_7P$	177263559	38.00
3	LPC 20 : 4	/20 : 4	528.2687	$C_{28}H_{52}NO_7P$	86924000	18.64

Table 8: Anti-inflammatory and cytotoxic activities (IC_{50} in μg/mL) of crab lipids.

Sample	Inhibition of NO production	SK-LU-1	HL-60	HT-29	HepG2	MCF7
TL	71.5 ± 4.41	89.7 ± 2.39	>100	>100	>100	97.3 ± 4.78
UPoL	>100	>100	>100	>100	>100	>100
PoL	68.6 ± 3.65	91.9 ± 3.32	85.4 ± 6.68	94.4 ± 5.18	95.8 ± 4.21	87.8 ± 6.15
L-NMMA	7.6 ± 0.57	—-	—-	—-	—-	—-
Ellipticine	—-	0.38 ± 0.03	0.42 ± 0.02	0.43 ± 0.04	0.51 ± 0.04	0.39 ± 0.04

TL: total lipid; UPoL: unpolar lipd; PoL: polar lipd

Table 8 shows that the crab total lipids had inhibitory effects on NO production in LPS-stimulated RAW 264.7 cells with an IC_{50} of 71.5 μg/mL. Notably, the polar lipid fraction displayed potent NO inhibitory activity with an IC_{50} of 68.6 μg/mL. The test cells remained healthy and cell viability was not affected according to the MTT colorimetric assay (data not shown). Ahmad et al. reported anti-inflammatory activities (IC_{50}) of seafood ranging from 64.6 to 306.4 μg/mL, with the lowest for octopus at 64.4 μg/mL and the highest for school prawn at 306.4 μg/mL. The anti-inflammatory activities of both crab total and polar lipids were comparable to those of octopus lipids [35].

3.4. Cytotoxic Activity toward Five Cancer Cell Lines. Herein, we report the cytotoxic activity of phospholipids toward cancer cell lines for the first time. The lipid fractions inhibited cancer cell lines with IC_{50} values ranging from 85.4 to 97.3 μg/mL. Among five cancer cell lines, the total lipids showed cytotoxicity toward the SK-LU-1 lung cancer and MCF7 breast cancer cell lines with IC_{50} values of 89.7 and 97.3 μg/mL, respectively. Notably, polar lipids showed high cytotoxicity toward five studied cell lines including SK-LU-1, HL-60, HT-29, HepG2, and MCF7 with IC_{50} values ranging from 85.4 to 95.8 μg/mL.

Marine organisms are a potential source of secondary metabolites that can be developed into cancer therapies [36]. In previous work, haemolymph collected from the walking legs of the *Dromia dehaani* crab was evaluated for cytotoxicity toward rhabdomyosarcoma, HepG2, A549, MCF-7, and HT-29 cell lines [37]. The IC_{50} values ranged from 75 to 100 μg/mL; the highest activity was exhibited toward the MCF-7 cell line. In other work, mangrove crab soup

inhibited growth of Jurkat leukemic T-lymphocyte cells in dose- and time-dependent manners [38]. Compared to these studies, the cytotoxicity of *S. paramamosain* polar lipids had an IC_{50} similar to that of crab haemolymph. We suggest that crab polar lipids merit further investigation as anticancer food supplements.

4. Conclusions

We report profiles of the composition and molecular forms of phospholipids obtained from the mud crab *S. paramamosain*. Six types of phospholipids containing 54 different molecular forms were identified. These molecules were mainly made of the C16 : 0; C18 : 0; C20 : 4; C20 : 5; and C22 : 6 fatty acids. Notably, different contents were measured for the 21 common fatty acids found in the lipid fraction. The variety of fatty acid composition created a high nutritional value of phospholipid which was widely used as a food additive in a range of products.

We also report, for the first time, anti-inflammatory and cytotoxic effects of crab lipid and phospholipid. The anti-inflammatory activities (IC_{50}) of the total and polar lipids were 71.5 and 68.6 μg/mL, respectively. The polar lipid sample containing phospholipids also presented high cytotoxic activity (IC_{50}) toward five cancer cell lines, ranging from 85.4 to 95.8 μg/mL. Thus, we suggest that crab polar lipids merit further investigation about function and bioactivities of each phospholipid class and furthermore evaluate potential application of phospholipids in the clinical therapy.

Data Availability

The data used to support the findings of this study are included within the article and the supplementary information file.

Conflicts of Interest

The authors declare that they have no conflicts of interest.

Acknowledgments

This research was funded by the Ministry of Agriculture and Rural Development (MARD) with the grant no. 16/2017HĐ/KHCN-VP belonging to the Agriculture and Aquaculture Biotechnology Program. The authors are grateful to Dr. Andrey B. Imbs and his group at Laboratory of Comparative Biochemistry, National Scientific Center of Marine Biology, Far-Eastern Branch of the Russian Academy of Sciences, 17 Palchevskogo str., Vladivostok 690041, Russian Federation.

Supplementary Materials

Figure 1S: HPLC-HRMS and fragmentations of alkenyl acyl PE 18:0p/20 : 5 (C43H76NO7P). Figure 2S: HPLC-HRMS and fragmentations of diacyl PE 16 : 0/22 : 6 and diacyl PE 18 : 1/20 : 5 (C43H74NO8P). Figure 3S: HPLC-HRMS and fragmentations of LPE 20 : 4 (C25H42NO7P). Figure 4S: HPLC-HRMS and fragmentations of PI 18 : 0/20 : 5 (C47H81O13P). Figure 5S: HPLC-HRMS (a) and fragmentations of PS 18 : 0/20 : 5 (C44H76NO10P). Figure 6S: HPLC-HRMS and fragmentations of PC 16 : 0/18 : 1 (C42H82NO8P). Figure 7S: HPLC-HRMS and fragmentations of LPC/20 : 5 (C28H48NO7P). (*Supplementary Materials*)

References

[1] C. P. Keenan, P. J. Davie, and D. L. Mann, "A revision of the genus *Scylla* de Haan, 1833 (Crustacea: Decapoda: Brachyura: portunidae)," *Raffles Bulletin of Zoology*, vol. 46, pp. 217–245, 1998.

[2] C. P. Keenan, "Aquaculture of the mud crab, genus Scylla—past, present, future," in *Mud Crab Aquaculture and Biology*, C. P. Keenan and A. Blackshaw, Eds., pp. 9–13, ACIAR, Proceedings, Canberra, Australia, 1999.

[3] J. Zhao, X. Wen, S. Li, D. Zhu, and Y. Li, "Effects of dietary lipid levels on growth, feed utilization, body composition and antioxidants of juvenile mud crab *Scylla paramamosain* (Estampador)," *Aquaculture*, vol. 435, pp. 200–206, 2015.

[4] C. Tantikitti, R. Kaonoona, and J. Pongmaneerat, "Fatty acid profiles and carotenoids accumulation in hepatopancreas and ovary of wild female mud crab (*Scylla paramamosain*, Estampador, 1949)," *Songklanakarin Journal of Science and Technology*, vol. 37, pp. 609–616, 2015.

[5] F. Meng, H. Gao, X. Tang et al., "Biochemical composition of pond-cultured vs. wild gravid female mud crab *Scylla paramamosain* in Hainan, China: evaluating the nutritional value of cultured mud crab," *Journal of Shellfish Research*, vol. 36, no. 2, pp. 445–452, 2017.

[6] A. Mohapatra, T. R. Rautray, A. K. Patra, V. Vijayan, and R. K. Mohanty, "Trace element-based food value evaluation in soft and hard shelled mud crabs," *Food and Chemical Toxicology*, vol. 47, no. 11, pp. 2730–2734, 2009.

[7] S. Techa and J. S. Chung, "Ecdysteroids eegulate the levels of Molt Inhibiting Hormone (MIH) expression in the blue crab," *Callinectes sapidus, PLos One*, vol. 10, 2015.

[8] A. Yasuda, M. Ikeda, and Y. Naya, "Analysis of hemolymph ecdysteroids in the crayfish *Procambarus clarkii* by high performance capillar," *Nippon Suisan Gakkaishi*, vol. 59, pp. 1793–1799, 1993.

[9] M. A. Suprayudi, T. Takeuchi, and K. Hamasaki, "Phospholipids effect on survival and molting synchronicity of larvae mud crab *Scylla serrata*," *HAYATI Journal of Biosciences*, vol. 19, no. 4, pp. 163–168, 2012.

[10] H. Xu, J. Wang, T. Han et al., "Effects of dietary phospholipids levels on growth performance, lipid metabolism, and antioxidant capacity of the early juvenile green mud crab, *Scylla paramamosain* (Estampador)," *Aquaculture Research*, vol. 50, no. 2, pp. 513–520, 2018.

[11] National Research Council, *Nutrient Requirements of Fish and Shrimp*, National Academies Press, Washington DC, 2011.

[12] P. R. Bowser and R. Rosemark, "Mortalities of cultured lobsters, homarus, associated with a molt death syndrome," *Aquaculture*, vol. 23, no. 1–4, pp. 11–18, 1981.

[13] G. Corraze, "Lipid nutrition," in *Nutrition and Feeding of Fish and Crustaceans*, J. Guillaume, S. Kaushik, P. Bergot, and K. Me´tailler, Eds., pp. 111–130, Springer Prarois, Chichester, England, 2001.

[14] R. Lordan, A. Tsoupras, and I. Zabetakis, "Phospholipids of animal and marine origin: structure, function, and anti-inflammatory properties," *Molecules*, vol. 22, no. 11, 1964 pages, 2017.

[15] E. Murru, S. Banni, and G. Carta, "Nutritional properties of dietary omega-3-enriched phospholipids," *BioMed Research International*, vol. 2013, Article ID 965417, 13 pages, 2013.

[16] D. K. Gaudry, L. A. Taylor, J. Kluth et al., "Effects of marine phospholipids extract on the lipid levels of metastatic and nonmetastatic prostate cancer patients," *International Scholarly Research Notices*, vol. 2014, Article ID 249204, 12 pages, 2014.

[17] D. K Gaudry, L. A. Taylor, M. Schneider, and U. Massing, "Health effects of dietary phospholipids," *Lipids in Health and Disease*, vol. 11, no. 1, p. 3, 2012.

[18] E. G. Bligh and W. J. Dyer, "A rapid method of total lipid extraction and purification," *Canadian Journal of Biochemistry and Physiology*, vol. 37, no. 8, pp. 911–917, 1959.

[19] Q. T. Tran, T. T. T. Le, M. Q. Pham et al., "Fatty acid, lipid classes and phospholipid molecular species composition of the marine clam *Meretrix lyrata* (Sowerby 1851) from Cua Lo beach, Nghe An province," *Vietnam. Molecules*, vol. 24, no. 5, p. 895, 2019.

[20] A. B. Imbs, L. P. T. Dang, V. G. Rybin, and V. I. Svetashev, "Fatty acid, lipid class, and phospholipid molecular species composition of the soft coral *Xenia* sp. (Nha trang bay, the south China sea, Vietnam)," *Lipids*, vol. 50, no. 6, pp. 575–589, 2015.

[21] W. Christie, "Equivalent chain-lengths of methyl ester derivatives of fatty acids on gas chromatography A reappraisal," *Journal of Chromatography A*, vol. 447, no. 3, pp. 305–314, 1988.

[22] S. Harrabi, W. Herchi, H. Kallel, P. Mayer, and S. Boukhchina, "Liquid chromatographic-mass spectrometric analysis of glycerophospholipids in corn oil," *Food Chemistry*, vol. 114, no. 2, pp. 712–716, 2009.

[23] S. Boukhchina, K. Sebai, A. Cherif, H. Kallel, and P. M. Mayer, "Identification of glycerophospholipids in rapeseed, olive, almond, and sunflower oils by LC–MS and LC–MS–MS," *Canadian Journal of Chemistry*, vol. 82, no. 7, pp. 1210–1215, 2004.

[24] T. Mosmann, "Rapid colorimetric assay for cellular growth and survival: application to proliferation and cytotoxicity assays," *Journal of Immunological Methods*, vol. 65, no. 1-2, pp. 55–63, 1983.

[25] A. Monks, D. Scudiero, P. Skehan et al., "Feasibility of a high-flux anticancer drug screen using a diverse panel of cultured human tumor cell lines," *JNCI Journal of the National Cancer Institute*, vol. 83, no. 11, pp. 757–766, 1991.

[26] K. Sundarrao, J. Tinkerame, C. Kaluwin, K. Singh, and T. Matsuoka, "Lipid content, fatty acid, and mineral composition of mud crabs (*Scylla serrata*) from Papua New Guinea," *Journal of Food Composition and Analysis*, vol. 4, no. 3, pp. 276–280, 1991.

[27] V. R. Alava, E. T. Quinitio, J. B. de Pedro, Z. G. A. Orosco, and M. Wille, "Reproductive performance, lipids and fatty acids of mud crab *Scylla serrata* (Forsskål) fed dietary lipid levels," *Aquaculture Research*, vol. 38, no. 14, pp. 1442–1451, 2007.

[28] S. Colantonio, J. T. Simpson, R. J. Fisher et al., "Quantitative analysis of phospholipids using nanostructured laser desorption ionization targets," *Lipids*, vol. 46, no. 5, pp. 469–477, 2011.

[29] B. Kalisch, P. Dörmann, and G. Hölzl, "DGDG and Glycolipids in Plants and Algae," *Lipids in Plant and Algae Development*, vol. 86, pp. p51–83, Springer, Berlin, Germany, 2016.

[30] Z.-Y. Liu, D.-Y. Zhou, Z.-X. Wu et al., "Extraction and detailed characterization of phospholipid-enriched oils from six species of edible clams," *Food Chemistry*, vol. 239, pp. 1175–1181, 2018.

[31] M. Kojima, T. Morisaki, K. Izuhara et al., "Lipopolysaccharide increases cyclo-oxygenase-2 expression in a colon carcinoma cell line through nuclear factor-κB activation," *Oncogene*, vol. 19, no. 9, pp. 1225–1231, 2000.

[32] Y. C. Park, G. Rimbach, C. Saliou, G. Valacchi, and L. Packer, "Activity of monomeric, dimeric, and trimeric flavonoids on NO production, TNF-α secretion, and NF-κB-dependent gene expression in RAW 264.7 macrophages," *FEBS Letters*, vol. 465, no. 2-3, pp. 93–97, 2000.

[33] J. MacMicking, Q.-w. Xie, and C. Nathan, "Nitric oxide and macrophage function," *Annual Review of Immunology*, vol. 15, no. 1, pp. 323–350, 1997.

[34] H. Ohshima and H. Bartsch, "Chronic infections and inflammatory processes as cancer risk factors: possible role of nitric oxide in carcinogenesis," *Mutation Research/Fundamental and Molecular Mechanisms of Mutagenesis*, vol. 305, no. 2, pp. 253–264, 1994.

[35] T. Ahmad, D. Rudd, M. Kotiw, L. Liu, and K. Benkendorff, "Correlation between fatty acid profile and anti-inflammatory activity in common Australian seafood by-products," *Marine Drugs*, vol. 17, no. 3, pp. 155–174, 2019.

[36] J. Jimeno, G. Faircloth, J. Sousa-Faro, P. Scheuer, and K. Rinehart, "New marine derived anticancer therapeuticsd─A journey from the sea to clinical trials," *Marine Drugs*, vol. 2, no. 1, pp. 14–29, 2004.

[37] E. R. Priya and S. Ravichandran, "Anticancer compounds of *Calappa calappa* L," *International Journal of Zoological Research*, vol. 11, no. 3, pp. 107–111, 2015.

[38] M. Mohamed, N. I. M Sani, A. Ismail, and N. F. Mokhtar, "Cytotoxicity and anti-cancer effect of mangrove crab (*Scylla serrata*) soup on human leukemic Jurkat cells," *European Journal of Pharmaceutical and Medical Research*, vol. 2, pp. 192–195, 2017.